

Modelling the initiation of bitumen-filled microfractures in immature, organic-rich carbonate mudrocks: The Maastrichtian source rocks of Jordan

Israa S. Abu-Mahfouz, First Author^{a,b,*}, Akbar N. Wicaksono, Co-First Author^a, Erdem Idiz^c, Joe Cartwright^c, J. Carlos Santamarina^a, Volker C. Vahrenkamp^a

^a Ali I. Al-Naimi Petroleum Engineering Research Centre, King Abdullah University of Science and Technology (KAUST), Thuwal, 23955, Saudi Arabia

^b Department of Geosciences, King Fahd University of Petroleum and Minerals (KFUPM), Dhahran, 31261, Saudi Arabia

^c Department of Earth Sciences, University of Oxford, Oxford, OX1 3AN, UK

ARTICLE INFO

Keywords:

Bitumen-filled microfractures
Overpressure
Stress distribution
Kerogen shape
Source rocks
Middle East

ABSTRACT

The initiation of bitumen-filled microfractures was analysed in the organic-rich Maastrichtian carbonate mudrocks of Jordan, which show great potential as source rocks and for a future unconventional hydrocarbon play. A modelling approach was performed to assess the possible scenarios causing horizontal small-scale (mm to cm in length) bitumen fractures (microfractures) at the immature stage. The aim was to back-calculate how much overpressure and bitumen generation was needed in the past to initiate horizontal microfracturing, comparing those simulated parameters with the actual generation potential from the source rock samples. The results show that the local overpressure resulting from the bitumen generation during early catagenesis was not high enough to initiate the microfracturing. We hypothesise that the increase of internal pressure was caused by the inability of the bitumen to be squeezed into the pore space during burial. The resulting overpressure induced a perturbation to the stable-state stress distribution around the kerogen boundary that eventually led to the initiation of horizontal microfractures along the tip of bitumen flakes. Subsequently, short-distance migration of bitumen and a significant decrease in pressure have prevailed in the study area. This proves that primary migration can occur long before the source rock reaches the oil or gas windows, at a comparatively shallow burial depth. This also indicates that the first framework pathways by the precursor horizontal microfractures may control the flow patterns of the hydrocarbons within source rocks. Understanding these factors is critical to predicting the impact of these microscale fractures on hydrocarbon expulsion and storage, and hence likely productivity of an analogous subsurface unconventional reservoir.

1. Introduction

Hydrocarbons, in the form of bitumen, have been documented within multiscale fracture sets in a few studies, including microfractures developed during early catagenesis (e.g., [Ryder et al., 2013](#); [Abu-Mahfouz et al., 2019, 2020](#)). Understanding the very first generation of these bitumen microfractures is critical, as they provide the first network of pathways during the primary migration of hydrocarbons and pore-matrix connection in unconventional reservoirs. In fact, the process of microfracturing in organic-rich source rocks due to hydrocarbon generation involves three main consequential stages: volume expansion, pressure increase, and microfracturing ([Lewan, 1987](#); [Ozkaya, 1988](#); [Ozkaya and Akbar, 1991](#); [Berg and Gangi, 1999](#); [Lash and Engelder,](#)

[2005](#); [Al Duhailan et al., 2013](#)). After expulsion pressure is released, the created microfractures might close again. However, under continued hydrocarbon generation they are likely to be pathways for secondary and later generation pulses.

The source rock deposits of the Maastrichtian age in Jordan provide an excellent opportunity to characterise and model the initiation of the bitumen-bearing horizontal microfractures formed before or at the very earliest maturation stages. Previous studies on these source rocks have focused on their organic matter enrichment, maturation, hydrocarbon potential, sedimentological, and paleoenvironmental implications (e.g., [Abed and Al-Aroui., 1994](#); [Abed et al., 2009](#); [Ali Hussein et al., 2014a](#); [März et al., 2016](#); [Hakimi et al., 2016, 2018](#)). Only very few studies have focused on the bitumen disseminated in the matrix and filling hosted

* Corresponding author. Geosciences Department, College of Petroleum Engineering and Geosciences (CPG), King Fahd University of Petroleum and Minerals (KFUPM), P.O. Box 5070, KFUPM, Dhahran, 31261 Saudi Arabia.

E-mail address: israa.abumahfouz@kfupm.edu.sa (I.S. Abu-Mahfouz).

<https://doi.org/10.1016/j.marpetgeo.2022.105700>

Received 20 February 2022; Received in revised form 12 April 2022; Accepted 14 April 2022

Available online 19 April 2022

0264-8172/© 2022 The Authors. Published by Elsevier Ltd. This is an open access article under the CC BY license (<http://creativecommons.org/licenses/by/4.0/>).

fractures (Abu-Mahfouz et al., 2019, 2020, 2022). Abu-Mahfouz et al. (2019) conducted a comprehensive geochemical investigation of bitumen fractures in these Upper Cretaceous Source Rocks and presented a conceptual model favouring the development of bitumen fractures by hydraulic fracturing. The hydraulic fracturing was interpreted to have resulted from fluid overpressure in the organic matter due to: (a) volume change due to bitumen generation, and (b) permeability destruction in the organic mudstone, preventing fluid loss. Although this source rock is immature, it is believed that the yield of this early expelled bitumen has been high enough to cause volume change that resulted in fracturing.

Here we try to test the conceptual model proposed by Abu-Mahfouz et al. (2019) using an integrated observational and modelling approach, building upon previous observations and results on bitumen horizontal microfractures in the Upper Cretaceous source rocks of Jordan. The present study aims to address the following key scientific questions: Was the volume change due to bitumen generation able to create enough pressure to initiate hydraulic fracturing? If not, then what are the other possible scenarios leading to microfracturing? Finally, what are the insights for primary migration more generally?

2. Geological framework and overview

The study area is located on the western border of the Arabian Plate, specifically on the central part of Jordan (Fig. 1a). During the Late Cretaceous–Eocene, Jordan was a broad, shallow shelf located on the southern margin of the Neo-Tethys Sea. Positioned on the western rim of the Arabian Plate, the study area was subjected to variable compressional to extensional tectonic stress fields, which greatly impacted the sedimentation and structures in Jordan (Abu-Jaber et al., 1989). The margin of the Arabian plate was reactivated in the Late Cretaceous due to intra-oceanic subduction on its northern and eastern sides, which led to the obduction of ophiolites (Sharland et al., 2001; Ziegler, 2001; Haq and Al-Qahtani, 2005; Abed, 2013). This caused regional scale loading and subsidence across the Arabian plate, creating extensive accommodation space for sediment. A maximum flooding event occurred during the Early Maastrichtian and was responsible for the generation of a

pelagic carbonate factory over the Arabian Plate. An open shelf environment developed in the central part of Jordan, laterally changing to deep-ramp and pelagic conditions towards the north (Powell and Moh'd, 2011). The deposition of these units was considerably influenced by NW-SE syn-sedimentary normal faults under a normal stress regime (Lüning and Kuss, 2014). Marine conditions were then terminated by tectonic uplift in the latest Eocene (Powell and Moh'd, 2011).

The Upper Cretaceous source rocks of Jordan are black to greyish-black, organic matter rich, bitumen-bearing marl to limestone layers (Abed and Aroui, 2006; Alnawafleh, 2007; Alnawafleh and Fraige, 2015; Alqudah et al., 2015; März et al., 2016; Beik et al., 2017; Abu-Mahfouz et al., 2019). They were deposited in shallow continental-shelf environments during the Maastrichtian-Late Eocene under environments that led to the deposition and preservation of organic matter: restricted water circulation, elevated salinity and anoxia (Abed et al., 2005; März et al., 2016; Beik et al., 2017).

The studied interval lies within the Belqa group and comprises three geological formations (from older to younger): The Al-Hisa Phosphorite Formation (AHP), which consists of phosphorite, chert, and bituminous marl; the Muwaqqar Chalk Marl Formation (MCM) mainly composed of bituminous marl with chert beds; and the Umm Rijam Chert-Limestone (URC) Formation consisting of alternating beds of chalky limestone and marl with abundant chert beds and nodules. Bitumen *sensu stricto* is operationally defined as the extractable portion of organic-rich rocks (see recent reviews by Pepper, 2017; Mastalerz et al., 2018 and Misch et al., 2019). Bitumen can be *pre-oil* (generated at very incipient cracking of kerogen) or *post-oil* (generated as a result of catagenesis) (Curiale, 1986; Jacob, 1989; Pepper, 2017; Mastalerz et al., 2018). Pepper (2017) defines *pre-oil* bitumen as “transitional with Organic Matter (OM)/kerogen” and as “organic matter (OM) whose structure has been mechanically weakened by bond breakage during maturation”. Such bitumens, rich in pre-asphaltene and asphaltene at the very early stages of maturity (Stainforth, 2009; He et al., 2022) are especially found in rocks with lower cracking thresholds, such as those containing S-rich kerogens, and are mobilized as a result of overburden load, often forming bitumen dykes (Curiale, 1986; Jacob, 1989; Pepper, 2017).

A previous study by Abu-Mahfouz et al. (2019) shows that the

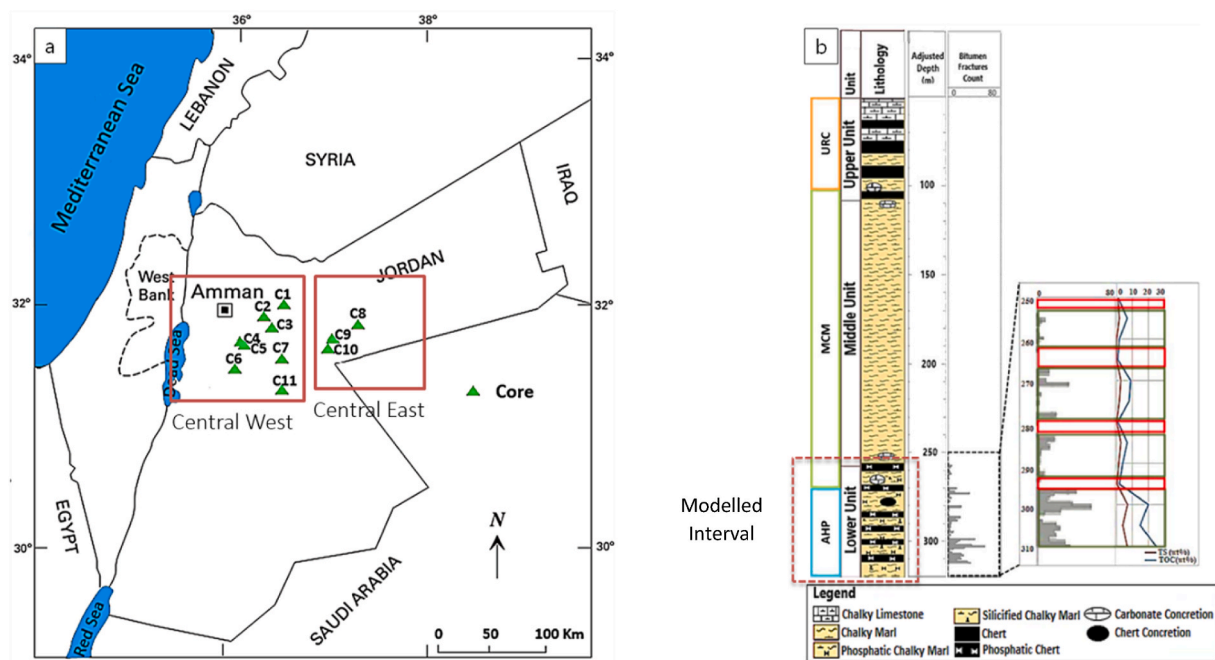


Fig. 1. a) Map of Jordan showing the location of the study area and cored wells. b) Generalised stratigraphic column of the study interval and a representative fracture log showing a high intensity of bitumen fractures/microfractures in the lower interval which has a positive correlation with TOC and sulfur contents (from Abu-Mahfouz et al., 2019).

bitumen fractures and micro-fractures are mainly concentrated at the base of the Upper Cretaceous (Maastrichtian) Muwaqqar Chalk Marl Formation, and have a positive correlation with Total Organic Carbon (TOC) and sulfur content (Fig. 1b). TOC content ranges from 3 to 30 wt% (Hakimi et al., 2016; Abu-Mahfouz et al., 2019, 2020). The Hydrogen Index (HI) and Rock-Eval T_{max} data suggest that organic matter is predominantly Type I/II S Kerogen, indicating a marine origin (Fig. 2). These Upper Cretaceous source rocks are immature. However, due to their high sulfur content (2–12 wt%), they could reach the bitumen generation window at an early stage of catagenesis (Abed et al., 2005; Hakimi et al., 2016; Sokol et al., 2017; Aljariri Alhesan et al., 2018; Abu-Mahfouz et al., 2019, 2020, 2022).

3. Methodology

A modelling approach was performed to assess the proposed conceptual model of horizontal bitumen microfracturing before the maturation stage. The idea is to back-calculate the overpressure and bitumen generation needed to initiate horizontal microfracturing, and then compare those simulated parameters with the actual generation potential from the source rock samples.

The lower interval of the Upper Cretaceous source rock in Jordan (the lower part of the MCM formation) was chosen for modelling as it hosts the most bitumen fractures and micro-fractures. Samples were collected from 11 cored wells from Central East and Central West Jordan (Fig. 1a). Microscopic investigation of thin sections was carried out to characterise the occurrence of microfractures, bitumen, and traces of kerogen using a LEICA DM 750P polarising light microscope. Selected samples were then investigated under Scanning Electron Microscope (SEM).

Backscattered electron (BSE) images were generated to characterise microfractures and examine their propagation direction. The geometry

of the kerogen traces was measured from petrography observation to have the representative geometrical characteristic of the kerogen body. Later, we simulated the stress concentration as a function of overpressure around the kerogen body. The point at which the total stress concentration is higher than the tensile strength of the rock marked the initiation of microfracturing. The amount of overpressure needed to reach this point was then recorded and compared with the actual overpressure generated based on the kinetic model of the source rock. The equations that are used to model the stress distribution along the kerogen body, and to calculate overpressure as a function of bitumen generation, are listed in Appendix 1 and Appendix 2 (see Supplementary Materials), respectively.

4. Results

4.1. Bitumen-filled microfractures and kerogen geometry

Microscopic (thin section and BSE images) analysis of the bituminous mudstone-wackestone interval was conducted to characterise the occurrence of bitumen-filled microfractures/filaments, and the original geometry of kerogen. Horizontal and sub-horizontal microfractures, filled with bitumen, are commonly observed. Fig. 3a shows an example of bitumen-bearing horizontal microfractures in the lower interval of the MCM Formation. The direction of the microfracture opening is perpendicular to the crack walls with a lack of shear offset, suggesting that the microfractures are mode-I cracks. This is also evidenced by the excellent match between the surfaces of the grains at both walls of the microfractures. EDS map data show that most microfractures are filled with bitumen, which is indicated by the high organic carbon content along the cracks (Fig. 3b). The bitumen can also be found as connected fine filaments disseminated in the matrix, as shown in Fig. 3c.

The geometry of the bitumen is a flattened elliptical shape that is

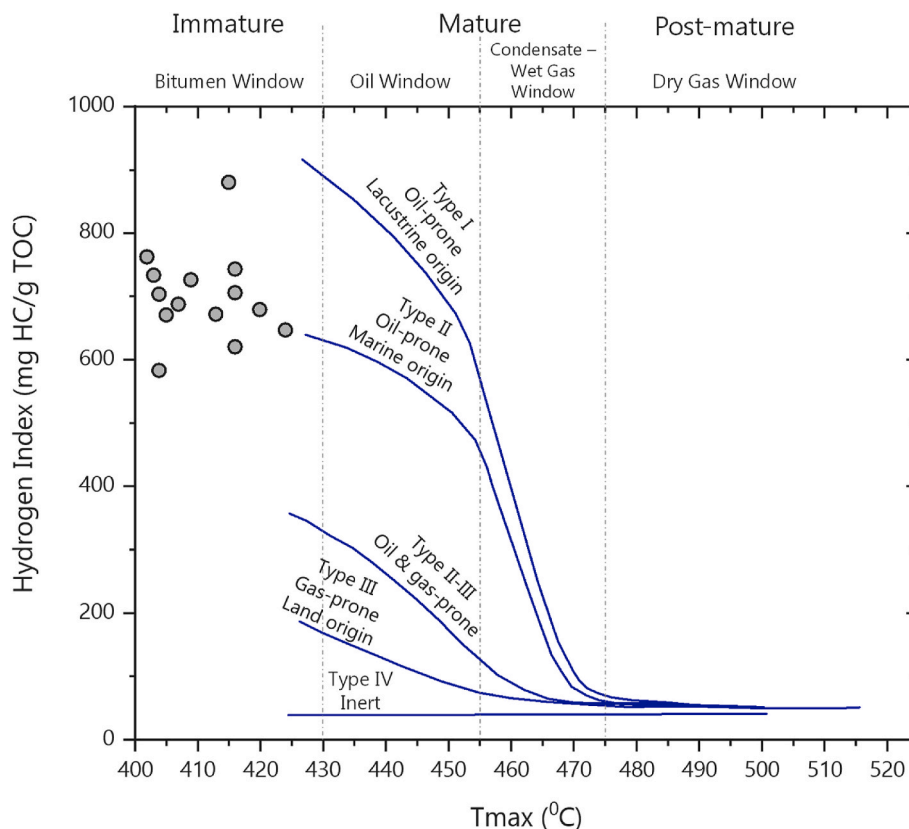


Fig. 2. Plot showing hydrogen index (HI) and Rock-Eval T_{max} data, suggesting that organic matter is dominantly Type I/II Kerogen and the rocks are immature (modified from Abu-Mahfouz et al., 2019).

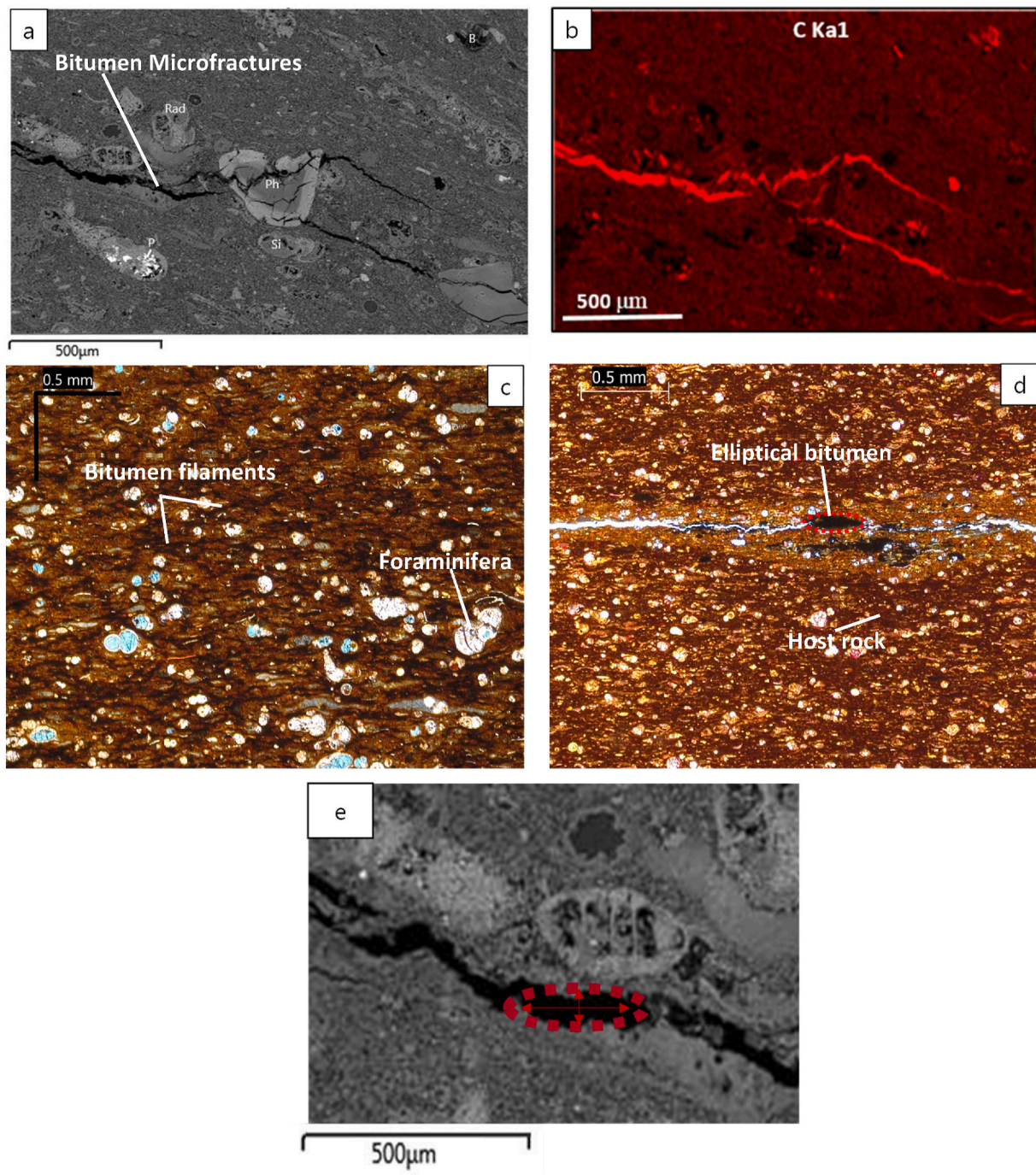


Fig. 3. a) BSE image of bitumen-bearing horizontal microfractures in the lower interval of study source rocks. b) EDS map showing carbon content in the bitumen microfracture and matrix. c) Connected bitumen-filled fine filaments in the matrix. d) Elliptical shape of bitumen along the microfracture (dashed red line). e) The geometry of the kerogen traces is characterised by measuring the aspect ratio: the ratio between the major and minor axis of an elliptical shape. Fig. 3a, b, and 3e are taken and modified from Abu-Mahfouz et al. (2019). (For interpretation of the references to colour in this figure legend, the reader is referred to the Web version of this article.)

mostly oriented subparallel to the bedding. In a few cases, bitumen is observed as small amorphous particles in irregular shapes. Fig. 3d and e provide an example of an elliptical shape of bitumen along a microfracture. These bitumen particles are suspected to represent the trace of the original shape of kerogen before the thermal cracking starts in early catagenesis.

The geometry of the kerogen traces is characterised by measuring the aspect ratio on the thin sections: the ratio between the major and minor axis of an elliptical shape, as shown in Fig. 3e. Over 278 kerogen traces have been identified and measured from the organic-rich bituminous

mudstone-wackestone interval, through samples coming from Central East and Central West areas, with an aspect ratio range from 1.7 to 9.6 (Fig. 4). The average value was used to represent the geometrical characteristics of the kerogen, which was then used as an input for the modelling efforts. The average aspect ratios are 4.1 and 4.7 for the Central East and Central West areas, respectively. It is also observed that there is no significant change in the actual size and aspect ratio with depth in both areas. This indicates that the load-bearing bitumen most likely failed to compact during burial.

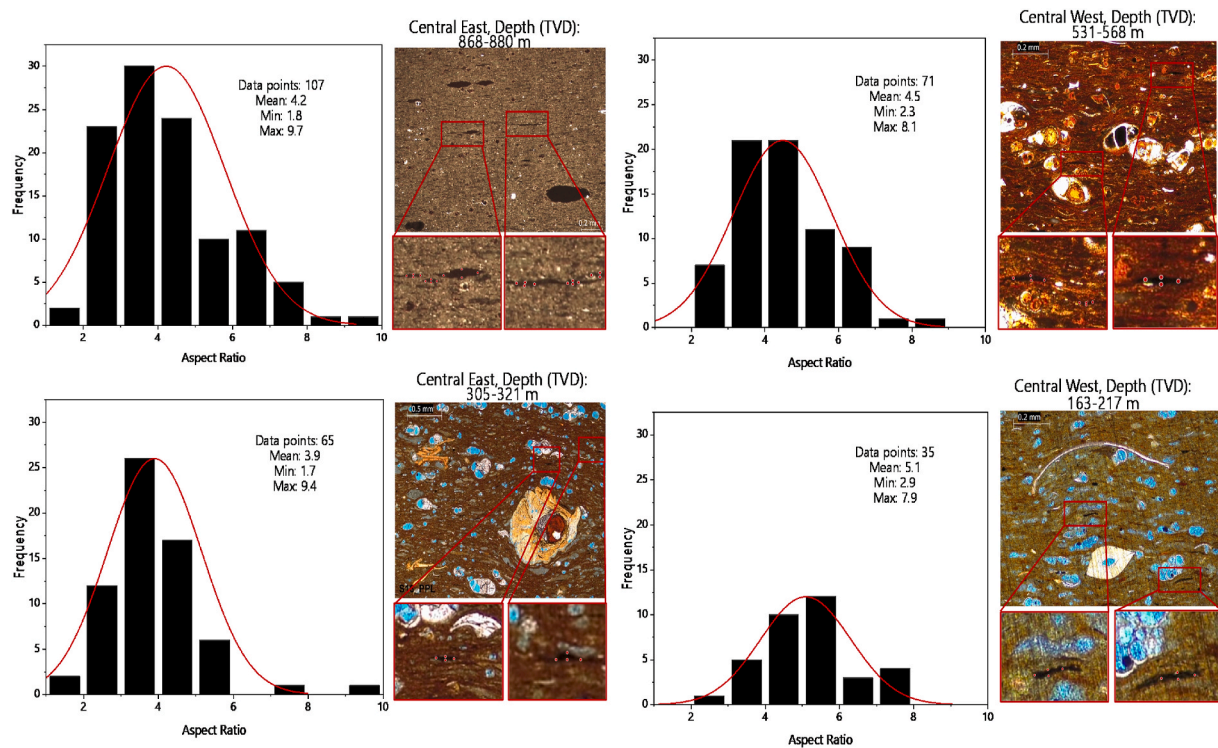


Fig. 4. Histogram showing the distribution of aspect ratio measurements of the kerogen traces, the corresponding summary statistic, and the representative thin sections, for each Central East and Central West area, lower and upper interval.

4.2. Back-calculation: how much overpressure is needed to generate microfractures?

The back-calculation is performed by modelling the stress distribution along the kerogen body during the first initiation of bitumen microfracturing. The kerogen body geometry is derived from the petrography observation. The kerogen body is of a flattened elliptical

shape and is being represented mathematically by the value of its aspect ratio. The depth and time of the first initiation of bitumen microfracturing for the Central East area were derived from the burial history and core data previously reported by Abu-Mahfouz et al. (2019). The abundance of fractures and the distribution of micro-to cm-scale bitumen fractures from core data are used as indicators to trace the onset depth of microfracturing into the burial history. The timing of

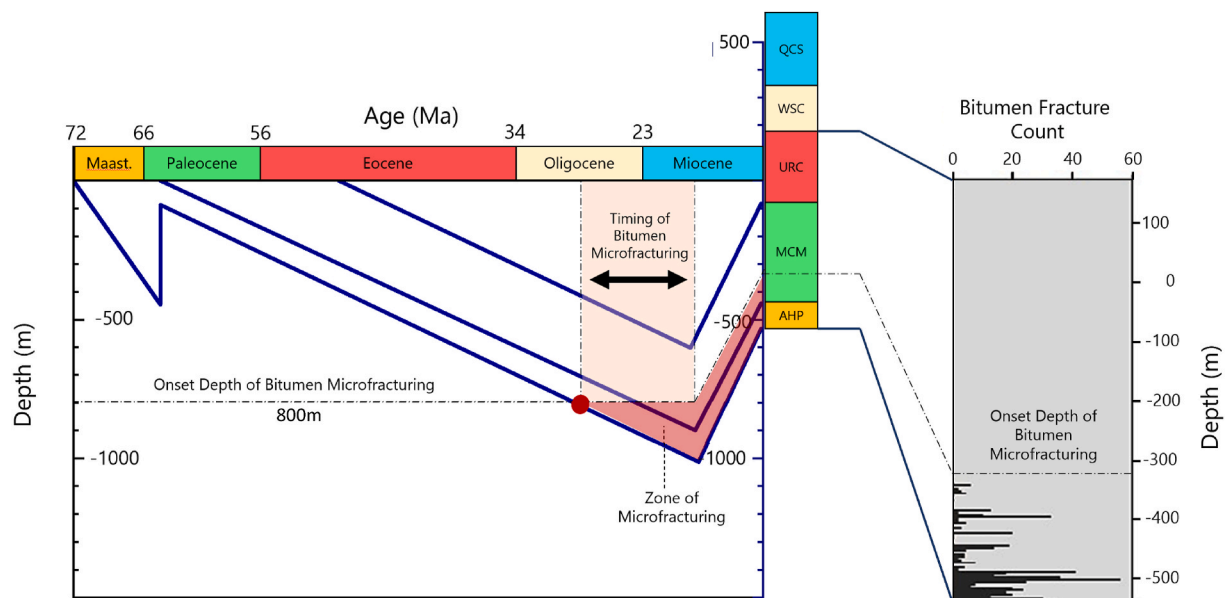


Fig. 5. The modelling of stress distribution is being done at the initiation point of microfracturing in the lower interval of MCM formation, approximately at -800 m burial depth during Oligocene, ~27 Ma (red circle point). The abundance of fractures and the distribution of micro-to cm-scale bitumen fractures from core data are used as indicators to trace the onset depth of microfracturing into the burial history. The timing of microfracturing was acquired using stable isotopes data and crosscutting relationships between bitumen microfractures and other mineralized fractures (Abu-Mahfouz, 2019; Hooker et al., 2019). (For interpretation of the references to colour in this figure legend, the reader is referred to the Web version of this article.)

microfracturing was estimated using stable isotope data and by analysing crosscutting relationships between bitumen microfractures and other mineralized fractures (Abu-Mahfouz, 2019; Hooker et al., 2019). The isotope dating results suggest that the timing of horizontal bitumen microfracturing occurred during Oligocene to Miocene, which is consistent with the depth inferred from the burial history. Finally, the modelling of stress distribution is performed at this initiation point of microfracturing in the lower interval of MCM formation, approximately at -800 m burial depth which was reached during the Oligocene (~ 27 Ma; Fig. 5). The equations and parameters used to generate the model are explained in Appendix 1.

The modelled stress distribution around the kerogen body as a function of overpressure is shown in Fig. 6. The figure shows the magnitude of tangential stress acting at any location along the kerogen boundary in a radial coordinate frame. At an overpressure of 8 MPa, the tangential stresses acting at the kerogen boundary were all in a compressive mode (positive value) and the stable state was still preserved. During this stage, the maximum tangential stress was distributed on the horizontal axis while the least stress was on the vertical axis of the elliptical kerogen. As we increased the magnitude of overpressure to 14.9 MPa, a perturbation on the stable state was observed. It lowered the maximum tangential stresses significantly to the point that it created a reversal of stress distribution. At this stage, the minimum tangential stress entered an extension regime (negative value) and was in the horizontal direction at the tip of the elliptical kerogen. The overpressure of 17 MPa marks the initiation of failure/fracturing, in which the minimum tangential stress exceeded the tensile strength of the rock. Since the failures are concentrated on the tip of the horizontal axis of the elliptical kerogen body, horizontal microfractures are generated. Once a microfracture is initiated, we suspect that pressure will decrease. The decrease in overpressure as microfractures continue to propagate during expulsion was not modelled in this study. Expulsion continued until maximum burial was reached and was then terminated by uplift. Nevertheless, the back-calculation analysis shows that at least 17 MPa of overpressure is needed to create horizontal microfractures and initiate the first expulsion.

4.3. Overpressure generated from kerogen to bitumen conversion during the immature stage

Bitumen generation from kerogen derives volume expansion relative to its original state. These volume changes create an increase in the internal pressure (overpressure), in addition to the hydrostatic pressure. The greater the fraction of kerogen transformed relative to its initial mass (here called transformation ratio, T_r), the higher the volume change that is created, and thus higher overpressure is generated. A

mass balance approach to calculate the overpressure as a function of transformation ratio is adapted from Berg and Gangi (1999), which is explained in detail in Appendix 2. The transformation ratio for the study source rock interval is derived from the bulk kinetic model previously reported by Hakimi et al. (2018) (Fig. 7). It estimates the transformation ratio based on the increase of temperature during the thermal cracking of the kerogen.

Overpressure was estimated from the initiation point of microfracturing (-800 m burial depth) until the maximum burial (-1000 m burial depth). This was undertaken to check whether the overpressure during bitumen generation reached the requisite overpressure needed to create microfracture. Assuming a range of gradient geothermal from 30° – 35° °C/km, a surface temperature of 25° °C, and burial from -800 m to -1000 m, the possible range of temperature during the thermal cracking is from 49° °C to 60° °C. This temperature range corresponds to a transformation ratio of 0.006–0.021 and maturity of 0.3–0.34 for the most sulfur-rich samples during the bitumen generation (Fig. 7). The overpressure calculation result shows that only 0.28 MPa–0.9 MPa of overpressure is generated due to the volume changes during kerogen to bitumen conversion (Fig. 8). Those values are considered very low compared to the pressures needed to stimulate the fracturing of around 17 MPa. It is estimated that a transformation ratio of at least 0.47–0.5 needs to be achieved to generate 17 MPa of overpressure and initiate fracturing from thermal cracking of kerogen conversion.

5. Discussion

5.1. Horizontal-microfracturing mechanisms

The modelling approaches used here prove that the observed horizontal microfractures cannot be only related to hydraulic fracturing that occurred due to the volume change during bitumen generation at early catagenesis. The overpressure resulting from the volume change was not high enough to initiate the microfracturing. Nevertheless, there must be another mechanism that increases the internal pressure of the bitumen which eventually leads to horizontal microfracturing. Thus, here we hypothesise that the increase of internal pressure was caused by the inability of the bitumen to move through the pore space during burial. The very low permeability of carbonate mudstone is suggested to have prevented the fluid loss and compaction of the bitumen. Because of this flow impediment and the resulting failure to compact, the internal pressure of the load-bearing bitumen increased to accommodate the increase in overburden loading during burial. The failure of bitumen compaction is evident from the kerogen geometry analysis. The aspect ratio and size of the kerogen traces or bitumen do not change with depth. This indicates that disequilibrium compaction has occurred in the past

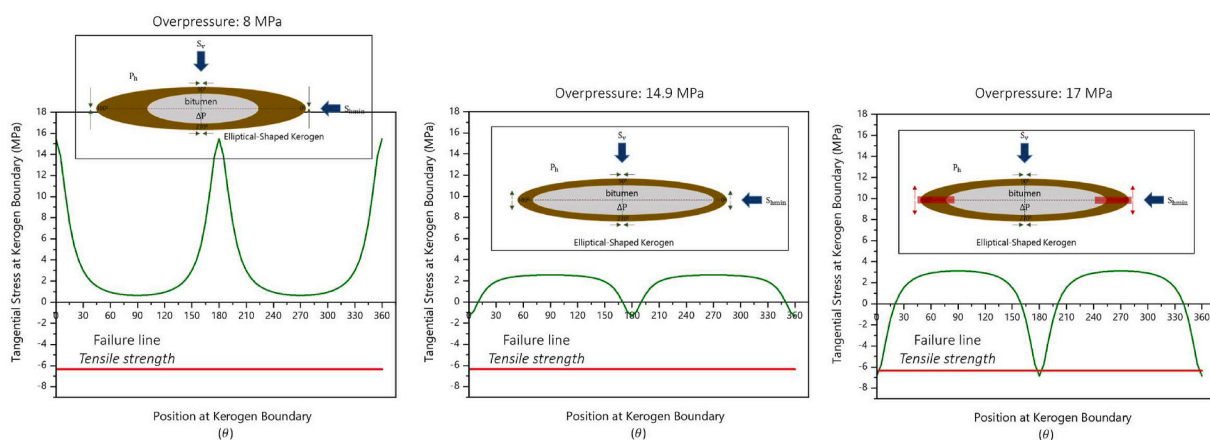


Fig. 6. The modelled stress distribution around the kerogen body as a function of overpressure. The figure shows the magnitude of tangential stress acting at any location along the kerogen boundary in a radial coordinate.

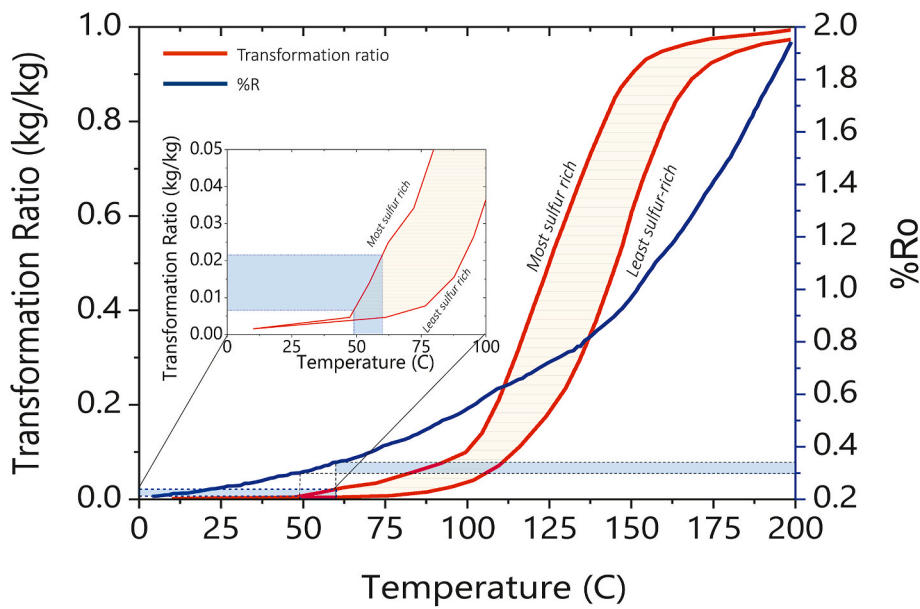


Fig. 7. Diagram showing the transformation ratio as a function of temperature for the Upper Cretaceous source rock in Jordan derived from the bulk kinetic model previously reported by Hakimi et al. (2018). The possible range of temperature during the thermal cracking is from 49 °C to 60 °C (shown in blue shades in the zoomed-in area). This temperature range corresponds to 0.006 to 0.021 of transformation ratio and maturity of 0.3–0.34 for the most sulfur-rich samples during the bitumen generation. (For interpretation of the references to colour in this figure legend, the reader is referred to the Web version of this article.)

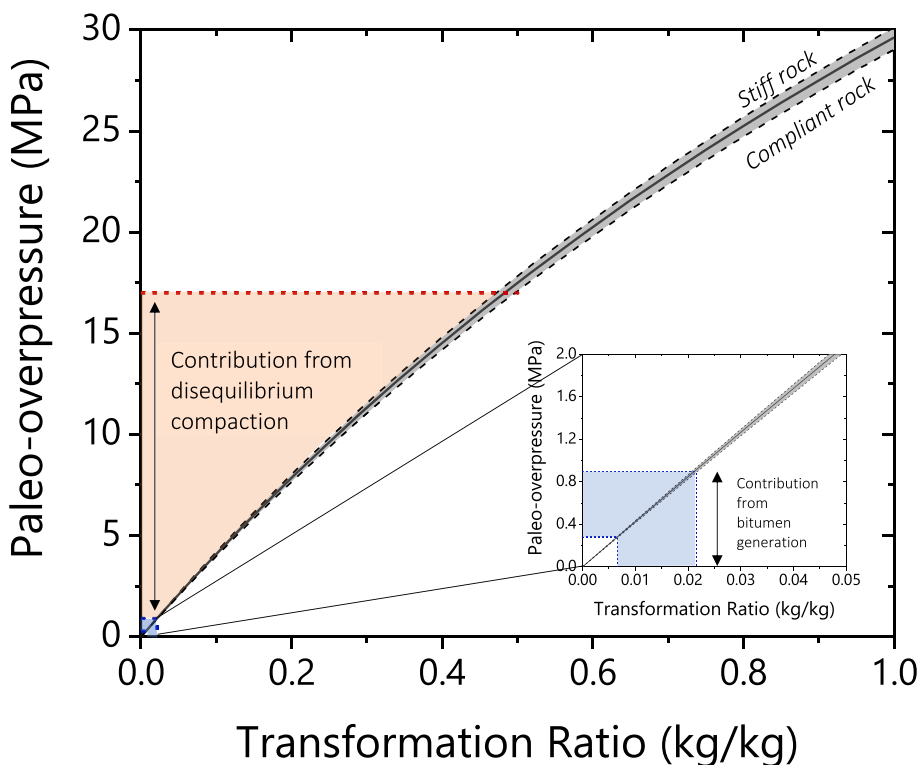


Fig. 8. Diagram showing the overpressure calculation results as a function of transformation ratio for the study source rock interval. Note that only 0.28 MPa–0.9 MPa of overpressure is generated due to the volume changes during kerogen to bitumen conversion. It is estimated that at least 0.47–0.5 of transformation ratio needs to be achieved to generate 17 MPa of overpressure and initiate fracturing from thermal cracking of kerogen conversion. The light brown-shaded area represents the overpressure caused by the compaction resulting from disequilibrium due to the very low permeability of the host rock. (For interpretation of the references to colour in this figure legend, the reader is referred to the Web version of this article.)

and caused more significant overpressure.

Fig. 9 summarizes the stages involved from the deposition up to the initiation of microfracturing in the Upper Cretaceous source rock in Jordan. During the Maastrichtian, a pelagic carbonate factory existed, with organic matter production by marine algae in the photic zone and caused by upwelling of nutrient-rich waters. Organic matter was preserved in anoxic conditions at the base of the basin and then transformed to kerogen. During the shallow burial stage (<500 m), mechanical compaction occurred, increasing the degree of flattening of the kerogen, and introducing anisotropy in the flattened elliptical kerogen shape. The observed wide spectrum of the aspect ratio of kerogen lenses from about 1.7 to 9.6 is believed here to reflect the variation of the original (pre-

compaction) shape of the kerogen, the degree of compaction, and the local influence of shielding by surrounding grains. The conversion of kerogen to bitumen at early catagenesis caused volume expansion, increasing the incremental pressure inside the kerogen cavities. At the same time, disequilibrium compaction had taken place due to the very low permeability of the host rock.

The overpressure generated by this process is believed to be much higher than from catagenesis. This paleo-overpressure induced a perturbation to the stable-state stress distribution around the kerogen boundary that eventually led to the initiation of horizontal microfractures along the tip of flattened-shaped kerogen as filaments. The propagation of these bitumen filaments is likely to have been controlled

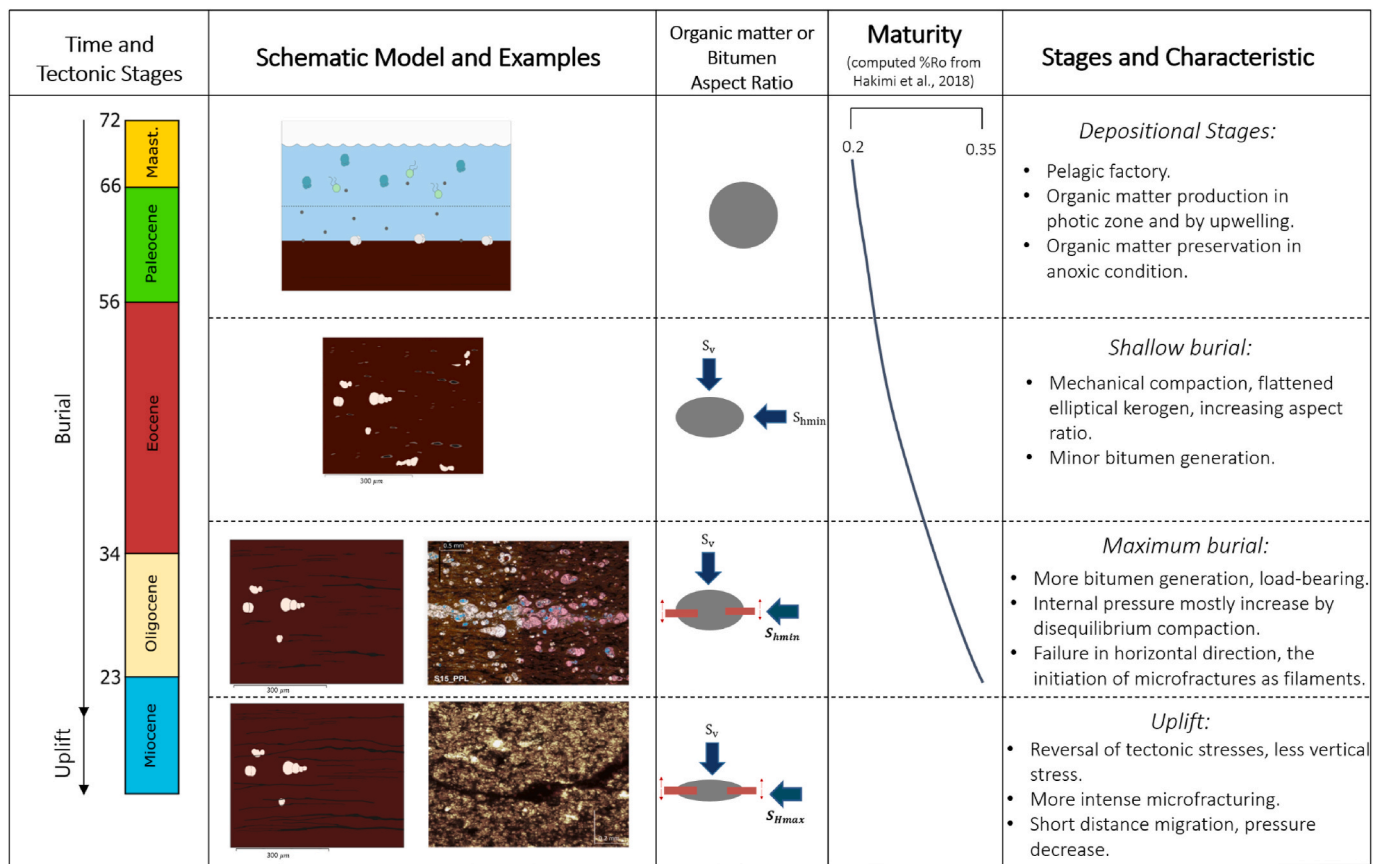


Fig. 9. A summary of the geological stages involved in the initiation of bitumen microfractures represented by a schematic model showing the different stages from the deposition to the initiation of bitumen microfractures in the Upper Cretaceous source rock of Jordan.

by the microfabric layering of the host rock. These filaments are suspected to be the initiation stage of crack propagation which then developed into more fully developed fractures.

Here we postulate that the change of principal stresses to a compressive regime during uplift is an important factor that supports the creation of open fractures. As the fracturing became more pronounced, the short-distance migration of bitumen leads to a significant decrease in overpressure.

A previous study by Abu-Mahfouz et al. (2019) shows that the biomarker signatures obtained from the matrix and fracture bitumens are identical, which indicates that they are sourced from the same type of organic matter. This great similarity in the biomarker patterns of the matrix bitumen and the solid bitumen found in microfractures provides another piece of evidence that fracture bitumen is local, derived from the same source rock.

5.2. Insights on the primary migration of bitumen

This study shows that the anisotropy in kerogen shape influences the orientation of microfracturing; the direction of initiation and propagation. Generally, in a normal stress regime, opening-mode fractures will propagate along a plane perpendicular to the minimum-compressive principal stress, normal to the plane of the crack, which is a vertical direction. However, in the case of the study source rocks, horizontal microfracturing is favoured due to the original relatively flattened-shaped kerogen. The shape of the kerogen dictates the stress distribution along its boundary, to the point that the minimum tangential stress falls within the horizontal direction and exceeds the tensile strength. This happened mainly because the increase in internal pressure accumulates at the tip of the elliptical shape horizontal axis and eventually acts against the effective overburden stress. The geometric form of the

organic particles concentrated in specific layers of laminated source rocks may influence the initiation of horizontal microfractures under a given stress system (Lash and Engelder, 2005). The more flattened, higher aspect ratio, the easier it is to reach failure and initiate microfracturing in the horizontal direction.

One of the main findings in this study is that the expulsion in the form of bitumen can occur at the earliest stages of kerogen cracking such as for sulfur-rich type II-S kerogen. The effects of overburden load on pre-asphaltene and/or asphaltene-rich bitumen leads to a significant overpressure that eventually initiates the horizontal microfracturing and the physical mobilization of bitumen that is not buoyancy driven. This means that the microfracture frameworks could also be possibly generated way before the petroleum system reaches the oil window, which is likely to be overlooked by many classical models. This study also indicates that the likelihood flow patterns during primary migration of the mature oil/gas will be dictated by the precursor horizontal microfractures. These insights on the timing and flow pattern of primary migration should be considered as conceptual inputs for petroleum system modelling with similar source rock characteristics.

6. Conclusions

The modelling approach used in this study shows that the overpressure resulting from the volume change during bitumen generation was not high enough to initiate the microfracturing. The significant amount of overpressure is related to the disequilibrium compaction of the bitumen during the burial stage. The horizontal direction of the opening-mode cracks observed under normal basinal stress was related to the variation of the aspect ratio of kerogen shape, which dictates the state of stress acting along the kerogen boundaries. Failure in the horizontal direction is favoured to be initiated along the tip of the flattened-

elliptical-shaped kerogen as filaments. These filaments are suspected to be the initiation stage of horizontal microfracture creation. The change of principal stresses to a compressive regime during the uplift stage had lowered the vertical stress and promoted more horizontal fracturing. Subsequently, short-distance migration of bitumen and a significant decrease in pressure have prevailed, implying that primary migration could occur way before the source rock reaches the oil/gas window, at a comparatively shallow burial (<500 m). This also indicates that the first framework pathways by the precursor horizontal microfractures will control the flow patterns of the hydrocarbons within the source rock. Understanding these factors is critical to predicting the impact of these microscale fractures on storage, and hence likely productivity of an analogous subsurface unconventional reservoir.

Declaration of competing interest

The authors declare that they have no known competing financial interests or personal relationships that could have appeared to influence the work reported in this paper.

Acknowledgements

This research was funded by the King Abdullah University of Science and Technology (KAUST) Endowment. The authors thank the Ministry of Energy and Mineral Resources (Jordan) for providing core samples from the cores drilled by Shell (represented by the Jordan Oil Shale Company (JOSCO)) in Jordan. We also thank Sander van den Boorn and John Stainforth for productive discussions. The reviewers Tiago M. Alves and the anonymous reviewer are sincerely thanked for the thorough and constructive comments on our original manuscript.

Appendix A. Supplementary data

Supplementary data to this article can be found online at <https://doi.org/10.1016/j.marpetgeo.2022.105700>.

References

- Abed, A.M., Al-Arouri, K., 1994. Organic geochemistry of central Jordan Upper Cretaceous phosphorites: phosphogenesis and source rock. In: *Proceedings of the 2nd International Conference – Geology of the Arab World*. Cairo University, Cairo, pp. 321–338.
- Abed, A.M., Arouri, K.R., Boreham, C.J., 2005. Source rock potential of the phosphorite bituminous chalk–marl sequence in Jordan. *Mar. Petrol. Geol.* 22, 413–425. <https://doi.org/10.1016/j.marpetgeo.2004.12.004>.
- Abed, A.M., Arouri, K., 2006. Characterisation and Genesis of Oil Shale from Jordan. Paper Rtos-A121 Presented at 'Recent Trends in Oil Shale': International Conference on Oils Shale, 7–9 November 2006 (Amman, Jordan).
- Abed, A.M., Arouri, K., Amiereh, B.S., Al-Hawari, Z., 2009. Characterisation and genesis of some Jordanian Oil shales. *Dirasat Pure Sci.* 36, 7–17.
- Abed, M.A., 2013. The eastern Mediterranean phosphorite giants: an interplay between tectonics and upwelling. *GeoArabia* 18 (2), 67–94.
- Abu-Jaber, N.S., Kimberly, M.M., Cavaroc, V.V., 1989. Mesozoic–Paleogene basin development within the eastern Mediterranean borderland. *J. Petrol. Geol.* 12, 419–436. <https://doi.org/10.1111/j.1747-5457.1989.tb00241.x>.
- Abu-Mahfouz, I.S., Cartwright, J., Idiz, E., Hooker, J.N., Robinson, S., Boorn, S.H.J.M., 2019. Genesis and role of bitumen in fracture development during early catagenesis. *Petrol. Geosci.* <https://doi.org/10.1144/petgeo2018-179> petgeo2018-179.
- Abu-Mahfouz, I.S., 2019. Genesis of Natural Fracture Systems in Mudrocks (Upper Cretaceous–Eocene), Jordan. Ph.D. thesis. University of Oxford, Oxford, UK, p. 409.
- Abu-Mahfouz, I.S., Cartwright, J., Idiz, E., Hooker, J.N., Robinson, S., 2020. Silica diagenesis promotes early primary hydrocarbon migration. *Geology* 48. <https://doi.org/10.1130/G47023.1>.
- Abu-Mahfouz, I.S., Gaus, G., Grohmann, S., Klaver, J., Cartwright, J., Idiz, E., Littke, R., Patzek, T., Urai, J.S., Vahrenkamp, V., 2022. Improved understanding of hydrocarbon expulsion and associated fracturing during successive stages of maturation: insights from the artificial maturation of organic-rich, immature to early mature source rocks. In: *International Petroleum Technology Conference and Exhibition*. <https://doi.org/10.2523/IPTC-21895-MS>. IPTC-21895-MS.
- Al-Duhailan, Mohammed, Sonnenberg, Stephen, Meckel, Lawrence, Meckel, L., 2013. Insights on Hydrocarbon-Generation Microfracturing in Organic-Rich Shales, pp. 95–106. <https://doi.org/10.1190/urtec2013-011>.
- Ali Hussein, M., Alqudah, M., Podlaha, O.G., van den Boorn, S., Kolonic, S., Mutterlose, J., 2014. Ichnofabrics of Eocene oil shales from central Jordan and their use for paleoenvironmental reconstructions. *GeoArabia* 19, 143–158.
- Aljariri Alhesan, J., Fei, Y., Marshall, M., Jackson, W., Qi, Y., Chaffee, A., Cassidy, P., 2018. Long time, low temperature pyrolysis of El-Lajjun oil shale. *J. Anal. Appl. Pyrol.* 130, 135–141. <https://doi.org/10.1016/j.jaap.2018.01.017>.
- Alnawafleh, H.M., 2007. Geological Factors Controlling the Variability of Maastrichtian Bituminous Rocks in Jordan. PhD thesis. University of Nottingham, Nottingham, UK.
- Alnawafleh, H.M., Fraige, F.Y., 2015. Analysis of selected oil shale samples from El-Lajjun, central Jordan. <https://doi.org/10.4236/gm.2015.53008> *Geomaterials* 5, 77–84.
- Alqudah, M., Ali Hussein, M., Van den Boorn, S., Podlaha, O., Mutterlose, J., 2015. Biostratigraphy and depositional setting of Maastrichtian–Eocene oil shales from Jordan. *Mar. Petrol. Geol.* 60, 87–104. <https://doi.org/10.1016/j.marpetgeo.2014.07.025>.
- Beik, I., Giraldo, G.V., Podlaha, O., Mutterlose, J., 2017. Microfacies and depositional environment of late cretaceous to early paleocene oil shales from Jordan. *Arabian J. Geosci.* 10. <https://doi.org/10.1007/s12517-017-3118-6>.
- Berg, R., Gangi, A.F., 1999. Primary migration by oil-generation microfracturing in low-permeability source rocks: application to the Austin chalk, Texas. *AAPG (Am. Assoc. Pet. Geol.) Bull.* 83 (5), 727–756. <https://doi.org/10.1306/E4FD2D6B-1732-11D7-8645000102C1865D>.
- Curiale, J.A., 1986. Origin of solid bitumens, with emphasis on biological marker results. *Org. Geochem.* 10 (1–3), 559–580.
- Hakimi, M.H., Abdullah, W.H., Alqudah, M., Makeen, Y.M., Mustapha, K.A., 2016. Organic geochemical and petrographic characteristics of the oil shales in the Lajjun area, Central Jordan: origin of organic matter input and preservation conditions. *Fuel* 181, 34–45. <https://doi.org/10.1016/j.fuel.2016.04.070>.
- Hakimi, M.H., Abdullah, W., Alqudah, M., Makeen, Y., Mustapha, K.A., Hatem, B., 2018. Pyrolysis analyses and bulk kinetic models of the Late Cretaceous oil shales in Jordan and their implications for early mature sulphur rich oil generation potential. *Mar. Petrol. Geol.* 91, 764–775. <https://doi.org/10.1016/j.marpetgeo.2018.01.036>.
- Haq, B., Al-Qahtani, A., 2005. Phanerozoic cycles of sea-level change on the Arabian platform. *GeoArabia* 10/2, 127–160.
- He, M., Wang, Z., Moldowan, M.J., Peters, K., 2022. Insights into catalytic effects of clay minerals on hydrocarbon composition of generated liquid products during oil cracking from laboratory pyrolysis experiments. *Org. Geochem.* 163, 104–331. <https://doi.org/10.1016/j.orggeochem.2021.104331>.
- Hooker, J.N., Abu-Mahfouz, I.S., Meng, Q., Cartwright, J., 2019. Fractures in mudrocks. Advances in constraining timing and understanding mechanisms. *J. Struct. Geol.* 125, 166–173. <https://doi.org/10.1016/j.jsg.2018.04.020>.
- Jacob, H., 1989. Classification, structure, genesis and practical importance of natural solid oil bitumen (“migrabitumen”). *Int. J. Coal Geol.* 11 (1), 65–79.
- Lash, Gary, Engelder, Terry, 2005. An analysis of horizontal microcracking during catagenesis: example from the Catskill delta complex. *AAPG Bull.* - AAPG BULL 89, 1433–1449. <https://doi.org/10.1306/05250504141>.
- Lewan, M.D., 1987. Petrographic study of primary petroleum migration in the Woodford Shale and related rocks. In: Doligez, B. (Ed.), *Migration of Hydrocarbons in Sedimentary Basins*. Paris. Editions Technip, pp. 113–130.
- Lünning, S., Kuss, J., 2014. Petroleum geology of Jordan. In: Marlow, L., Kendall, C., Yose, L. (Eds.), *Petroleum Systems of the Tethyan Region*, vol. 106. AAPG Memoirs, pp. 217–239.
- März, C., Wagner, T., et al., 2016. Repeated enrichment of trace metals and organic carbon on an Eocene high-energy shelf caused by anoxia and reworking. *Geology* 44, 1011–1014. <https://doi.org/10.1130/G38412.1>.
- Mastalerz, M., Drobniak, A., Stankiewicz, A.B., 2018. Origin, properties, and implications of solid bitumen in source-rock reservoirs: a review. *Int. J. Coal Geol.* 195, 14–36.
- Misch, D., Gross, D., Hawranek, G., Horsfield, B., Klaver, J., Mendez-Martin, F., Urai, J. L., Vranjes-Wessely, S., Sachsenhofer, R.F., Schmatz, J., Li, J., 2019. Solid bitumen in shales: petrographic characteristics and implications for reservoir characterization. *Int. J. Coal Geol.* 205, 4–31.
- Ozkaya, I., 1988. A simple analysis of oil-induced fracturing in sedimentary rocks. *Mar. Petrol. Geol.* 5, 293–297.
- Ozkaya, I., Akbar, A., 1991. An iterative procedure to determine depth and time of primary oil migration and expulsion efficiency of source rocks. *J. Petrol. Sci. Eng.* 5, 371–378.
- Pepper, A., 2017. April. Definition, Modes of Occurrence and Pitfalls in Understanding the Term ‘bitumen’ in Conventional and Unconventional Petroleum Systems. American Association of Petroleum Geologists Annual Convention and Exhibition, pp. 2–5.
- Powell, J., Moh'd, B., 2011. Evolution of Cretaceous to Eocene alluvial and carbonate platform sequences in central and south Jordan. *GeoArabia* 16, 29–82.
- Ryder, R.T., Hackley, P.C., Trippi, M.H., Alimi, H., 2013. Evaluation of thermal maturity in the low maturity Devonian shales of the northern Appalachian Basin. In: AAPG Search and Discovery Article 10477, Parts 1 and 2, Presented at the AAPG Eastern Section Meeting, 25–29 September 2010. Kalamazoo, Michigan, USA. http://www.searchanddiscovery.com/documents/2013/10477ryder/ndx_ryder.
- Sokol, E.V., Kozmenko, O.A., et al., 2017. Calcareous sediments of the Muwaqqar chalk marl formation, Jordan: mineralogical and geochemical evidences for Zn and Cd enrichment. *Gondwana Res.* 46, 204–226. <https://doi.org/10.1016/j.gr.2017.03.008>.

- Stainforth, J.G., 2009. Practical kinetic modelling of petroleum generation and expulsion. *Mar. Petrol. Geol.* 26 (4), 552–572.
- Sharland, P.R., Archer, R., Casey, D.M., Davies, R.B., Hall, S.H., Heward, A.P., Horbury, A.D., Simmons, M.D., 2001. Arabian Plate Sequence Stratigraphy, vol. 2. GeoArabia special publication, Bahrain, p. 371.
- Ziegler, M., 2001. Late permian to holocene paleofacies evolution of the Arabian plate and its hydrocarbon occurrences. *GeoArabia* 6 (3), 445–504.